International Journal of Waste Resources

El-Saied et al., Int J Waste Resour 2017, 7:4
DOI: 10.4172/2252-5211.1000305

Research Article Open Access

Removal of Lead and Copper Ions from Polluted Aqueous Solutions using Nano-Sawdust Particles

Fathy El-Saied A*, Saeyda Abo-Elenan A and Fathia El-shinawy H

Chemistry Department, Menoufia University, Shebin El-Kom, Egypt

Abstract

Heavy metals pollution was considered as one of the most serious environmental problems. The removal of heavy metals ions (Pb^{2+} and Cu^{2+}) from dilute aqueous solutions was investigated by using biomaterials like nano-sawdust particles as bio-sorbent. The nano-sawdust was prepared and identified by (SEM), (TEM) and (FTIR) spectroscopy. Results of SEM study showed that the surface of sawdust has many pores with nano size in rang of (40-51 nm). The TEM image suggests that the produced material consists of nano particles. The FTIR gave characteristic bands due to presence of OH, NH_2 and C=O groups. The batch experiment indicates that the maximum bio-sorption efficiency for Pb^{2+} was 100% at optimum conditions of, pH 6, contact time 40 min and bio-sorbent dosage 2.0 g. However nano-sawdust gave removal efficiency 98.78% of Cu^{2+} under optimum conditions of, pH 7, contact time 50 min and bio-sorbent dosage 1.0 g. Kinetic studies indicated that the biosorption of Pb(II) and Cu(II) ions onto nono-sawdust was pseudo-second order.

Keywords: Nano–sawdust; Bio-sorption; Heavy metals; Batch experiments; Kinetic; Isotherms

Introduction

Many serious environmental problems were arised from the presence of heavy metals in the industrial waste water attributed to their non-biodegradable properties and toxicity [1]. Exposed to toxic heavy metals (Pb, Cu, Hg), even at low concentration lead to a wide range of spectrum health problems, such as convulsions, capillary, hepatic and renal damage. Precipitation, membrane processes, electrolytic recovery, liquid-liquid extraction, ion exchange and adsorption are techniques employed to the removal of heavy metals [2-4]. These techniques are ineffective or expensive, especially when the heavy metal ions are present in high concentration in the polluted media. Biosorption occurs due to chemico-physical interactions of metal ions with active groups such as carboxylic, phosphate, sulfate, amino, amide and hydroxyl groups [5,6]. Sawdust is one of agricultural waste materials that are available in large quantities, has low cost, easily regenerated after use and may have potential as inexpensive adsorbents. The mechanism of adsorption by sawdust is supposed by the active sites existing in the cellulose structure of sawdust and an ion exchange mechanism of adsorption by replacing protons of hydroxyl groups by metal ions [7]. Nano-fiber mats have agreat advantages, such as high porosity, high gas permeability, and high specific surface area per unit mass, which lead to a high adsorption capacity. The efficiency the chitosan electrospun nanofiber to adsorb Cu(II) ions was 6 and 11 times higher than that reported by chitosan microsphere and the plain chitosan [8]. The aim of the present work is to prepare nano-sawdust particles as a bio sorbent and evaluate the potential of using the prepared nano-sawdust particles as an adsorbent for removal of Pb^{2+} and Cu^{2+} ions from polluted aqueous media. The factors that affect adsorption capacity such as pH, contact time and the initial metal concentration were investigated to optimize the adsorption process. Langmuir and Freundlich isotherm models were used to simulate the adsorption characterization. The sorption kinetics was also investigated.

Materials and Methods

Preparation of nano-sawdust

Sawdust collected from carpentry workshop in Menoufia Governorate, Egypt. It was washed with distilled water to remove surface impurities and dried at 80°C for 24 h. Nano sawdust was prepared by the acid hydrolysis, which was carried out by sulphuric acid (H_2SO_4) solution 60 wt% at 45°C, 30 min under continuous agitation. The produced nano-sawdust was washed with distilled water several times up to constant pH, and then dried at 80°C for 24 h. The functional groups of the prepared bio-sorbent were characterized by using a Shimadzu Fourier Transform Infrared Spectrophotometer (FTIR system-BX 0.8009) with the range of 200–4000 cm^{-1}. Surface size was analyzed by a Scanning Electron Microscope (SEM,) (JSM-5300, JEOL Ltd.). An ion sputtering coating device (JEOL-JFC-1100E) was used to coat the SEM specimens with gold to increase the conductivity. The size of bio-sorbent was measured by JEOl Jem-1230 Transmission Electron Microscope.

Chemicals and reagents

The aqueous solutions of metal ions used in the present investigation were prepared by using analytical grade chemicals. Individual stock Cu(II) and Pb(II) solutions of 1000 mg metal ion/L concentration were prepared from $CuSO_4.5H_2O$ and $Pb(NO_3)_2$ respectively. These stock solutions were used to prepare a series of dilute solutions. The pH of solutions in range of 2-8 was adjusted by using 1.0 M hydrochloric acid solution and 1.0 M anhydrous sodium acetate solution. The pH-value of resulting solutions was measured by a pH meter, WTW-inolab, Germany. The metal concentrations in aqueous solutions were determined by Flame Atomic Absorption Spectrophotometer (FAAS) (Perkin Elmer 503) using a calibration curve prepared with standard metal ion solutions.

Batch adsorption study

Batch adsorption experiments were carried out to assessment

***Corresponding author:** Fathy El-Saied A, Chemistry Department, Faculty of Science, Menoufia University, Shebin El-Kom, Egypt, Tel: +20482222170; E-mail: elsayedfathy139@yahoo.com

Received September 29, 2017; **Accepted** October 09, 2017; **Published** October 16, 2017

Citation: El-Saied FA, Abo-Elenan SA, El-shinawy FH (2017) Removal of Lead and Copper Ions from Polluted Aqueous Solutions using Nano-Sawdust Particles. Int J Waste Resour 7: 305. doi: 10.4172/2252-5211.1000305

Citation: El-Saied FA, Abo-Elenan SA, El-shinawy FH (2017) Removal of Lead and Copper Ions from Polluted Aqueous Solutions using Nano-Sawdust Particles. Int J Waste Resour 7: 305. doi: 10.4172/2252-5211.1000305

the effect of various adsorption parameters such as pH, contact time, dosage of adsorbent and initial concentration of metal ions on the adsorption capacity of removal of metal ions (Pb^{2+} and Cu^{2+}) by using nano-sawdust to conduct the optimum adsorption parameters.

Effect of initial solution pH: The effect of pH on removal of metal ions by nano-sawdust was studied by changing the initial pH (2-8) of 50 ml of metal aqueous solution at concentration 5 mg/L by adjusting the value of pH with 1.0 M HCl and 1.0 M sodium acetate. 0.4 g of nano-sawdust was added to the solution in 100 ml flask. The mixture was shaken on magnetic stirrer at 300 rpm for 30 min at room temperature (25°C). The mixture was filtered then; the residual un-adsorbed metal ion in the filtrates was measured by AAS. Note that the pH of the aqueous solution was measured by the pH.

Effect of contact time: The effect of contact time on removal of metal ions was studied for varying contact times (10, 20, 30, 40, 50, 60, 90 and 120 min.). Experiments were carried out on a number of solutions each of them was composed of 50 ml of metal ion solution of 5 mg/L concentration at pH adjusted to the optimal pH then, 0.4 g of nano-sawdust was added to each solution. The solutions mixtures were shaken on a magnetic stirrer at 300 rpm for changing times (10-120) min. at room temperature (25˚C).

Effect of adsorbent dosage: Different dosages of the adsorbent (0.2-2 g) were added to a number of flasks each of them was contained 50 mL of metal aqueous solution of 5 mg/L concentration and adjusted to the optimal pH. The solutions mixtures were shaken on a magnetic stirrer at 300 rpm for the optimal contact time at room temperature (25ºC).

Effect of initial metals ions concentrations: Different metal ions concentrations over the range 1-13 mg/L were prepared in different conical flasks containing 50 ml of each concentration. Experiments were carried out at optimal conditions of pH of solution, contact time and dosage of the adsorbent.

After each experiment, the suspensions were filtered off using 0.45 µm membrane filter paper and the residual unabsorbed concentrations of metal ions in the filtrates were analyzed using Atomic Absorption Spectrophotometer (AAS).

Data analysis: The percentage of metal ions (R %) removed was calculated from equation:

$$R\% = (C_o - C_e / C_o) \times 100 \quad (1)$$

Where C0 is the initial concentration (mg/L) of the metal ion before adsorption and Ce is the concentration (mg/L) of metal ion at equilibrium.

The amount of metal ion (qt at time t) adsorbed per unit mass of the adsorbent (M) was evaluated by using the following equation:

$$q_t = (C_o - C_t)V / M \quad (2)$$

Ct is the concentration (mg/L) of metal ion after time t min., V is the volume of initial metal ion in liter and M the mass of adsorbent in gram

The adsorption capacity (qe) was determined using the mass balance equation:

$$q_e = (C_o - C_e)V/M \quad (3)$$

4.3.6 Kinetic analysis: The kinetics of adsorption was determined by analyzing adsorptive uptake of heavy metals from the aqueous metal solution at different time intervals. The pseudo-first-order and pseudo-second-order model equations are fitted to model the kinetics of heavy metals adsorption onto nano sawdust. The linearity of each model when plotted indicates whether the model suitably described the adsorption process or not. The pseudo-first-order equation is generally expressed as [9,10]

$$\ln(q_e - q_t) = \ln q_e - K_1 t \quad (4)$$

Where qe and qt are the sorption capacities at equilibrium and at time t, respectively ($mg.g^{-1}$) and k1 is the rate constant of pseudo-first order sorption ($L.min^{-1}$).

The pseudo- second-order equation is generally expressed as [11,12]

$$t/q_t = (1/K_2 q_e^2) + (t/q_e) \quad (5)$$

Where qe and qt are the sorption capacity at equilibrium and at time t, ($mg.g^{-1}$) respectively and k_2 is the rate constant of the pseudo-second order sorption ($g.mg^{-1}.min^{-1}$).

Adsorption isotherm experiments: Adsorption isotherm studies were carried out on the data of initial metal ions concentrations. The results were fitted to the commonly-used Langmuir and Freundlich isotherms.

Linear form of Langmuir isotherm equation is given as:

$$C_e/q_e = 1/(q_{max} KL) + (1/q_{max}) C_e \quad (6)$$

Where K_L is Langmuir equilibrium constant ($L.mg^{-1}$), and q_{max} ($mg.g^{-1}$) is the monolayer adsorption capacity. Langmuir isotherm can be characterized by a dimensionless constant separation factor (R_L) [13,14].

$$R_L = 1/[1 + (K_L \times C_o)] \quad (7)$$

Where Co in this case is the highest initial solute concentration. The value of separation factor (R_L) indicates the type of the isotherm and the nature of the adsorption process either to be unfavorable ($R_L<0$), linear ($R_L=1$), favorable ($0<R_L<1$) or irreversible ($R_L=0$).

Linear form of freundlich isotherm equation is given as:

$$\log q_e = \log K_F + (1/n) \log C_e \quad (8)$$

Where K_F ($L.g^{-1}$) is Freundlich adsorption isotherm constant and indicator of the multilayer adsorption capacity, 1/n is the adsorption intensity. The value of 1 /n (indicative of favorability when ($0.1<1/n<1$) [15].

Multi-components system

The effect of adsorbent dosage on the removal of lead and copper ions present together in the same aqueous solution was investigated at dosages (0.5, 1, 1.5 and 2 g). The experiment was carried out at controlled conditions, pH (6.5), 1 h contact time, temperature = 25°C and 300 rpm.

Industrial wastewater

The wastewater sample used was collected from the Industrial Area, Quesna, Menoufia Governorate, Egypt. It was carefully bottled in a plastic container and taken to the laboratory for analysis. Wastewater was filtered off using 0.45 µm membranes. The wastewater sample was analyzed by the Atomic-Absorption Spectrophotometer to determine the concentrations of $Pb^{2+}$and Cu^{2+} ions. In the experiment, 2.0 g of nano-sawdust was added to 50 mL of wastewater and shaken on a magnetic stirrer at 300 rpm at room temperature (25°C) for 1 hour at pH 6.5. Suspensions were filtered off using 0.45 µm membrane filter paper and kept for metal analyses.

Results and Discussion

Characterization of nano-sawdust bio-sorbent

Figure 1 shows the TEM image of the nano-sawdust sample. The TEM image indicates that the particles are spherical, uniform and mono-dispersed with an average size of (3 to 4 nm).

The SEM micrograph of nano-sawdust was carried out to analyze surface morphology. Figure 2, the SEM image shows that the surface of nano-sawdust has irregularly shaped pores.

Nano-sawdust is considered one of plant fibers which contain cellulose, hemicellulose and lignin. These components are primarily composed of alkanes, esters, aromatics, ketones and alcohols with different oxygen containing functional groups. Figure 3 shows FTIR spectra of free unloaded nano-sawdust (A) and loaded with metal ion nano-sawdust (B). Table 1 gives the assignments for the different functional groups. The strong peak at 3419 cm-1 due to stretching of overlapped amine and hydroxyl groups. Peaks at 1640 and 1511 cm^{-1} are corresponding to C=O and C=C of α-β unsaturated ketones. The observed peaks at 1269 and 1161 cm^{-1} due to C-O-C stretch of ester and lactones. Also the spectrum shows peaks at 2900, 1427 and 1375 cm^{-1} due to stretching and binding of C-H of alkyl group. The bands which located at 1454 cm^{-1} and (1111, 1050 cm^{-1}) are NH bond and C-OH stretch.

The FTIR spectrum of the free unloaded nano-sawdust and that of the loaded nano-sawdust after adsorption were compared. The comparison showed that the bandes characteristic to amides and hydroxyl groups at 3419 cm^{-1} and that characteristic to alkenes and aromatic protons at 2900 cm^{-1} were slightly shifted to lower frequencies. The Figure 3 shows also the bandes corresponding to nitriles, C=O and conjugated C=O , C=C and C-O were strongly shifted to lower frequencies. This indicates that thes functional groups are participated in the process of adsorption of metal ions.

Functional group	Stretches	cm^{-1}
Amine/hydroxyl	N-H stretch and O-H stretch	3419
Alkenes, aromatics	C-H stretch	2900
Nitriles	CN stretch vibration	2127
Amides and lactones	C=O stretch vibration	1641
Conjugated Phenyl Ketones	C=O conjugated	1511
Alkenes and aromatics	C=C bond	1427
Esters, amides and ketones	C-O stretch	1375
Alkyl groups	C-H deformation	1050

Table 1: FTIR spectral bands of nano-sawdust before loading with metal ion and their assignment.

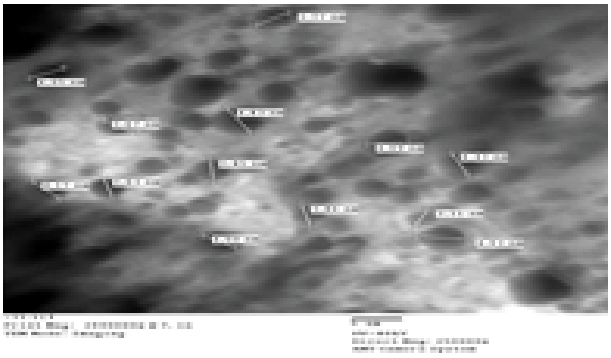

Figure 1: TEM image of nano-sawdust.

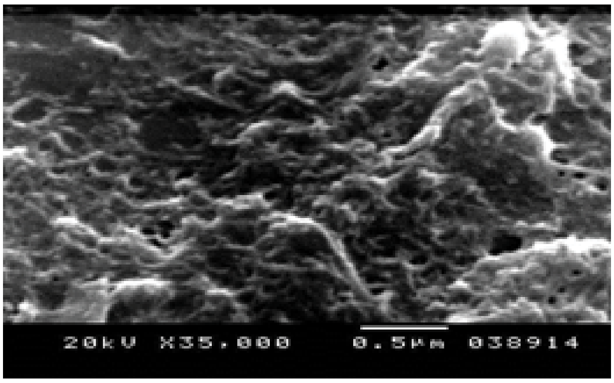

Figure 2: SEM micrograph image of nano-sawdust.

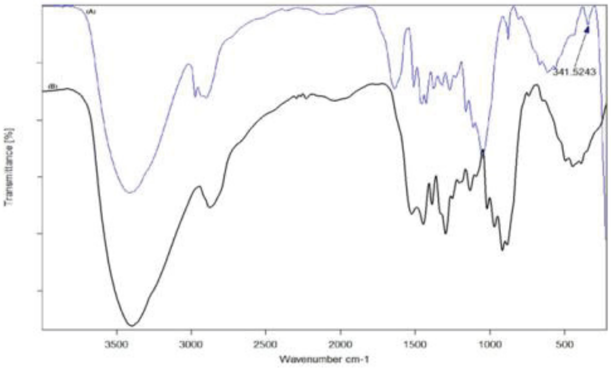

Figure 3: FTIR of free unloaded nano-sawdust and loaded with metal ion nano-sawdust after biosorption.

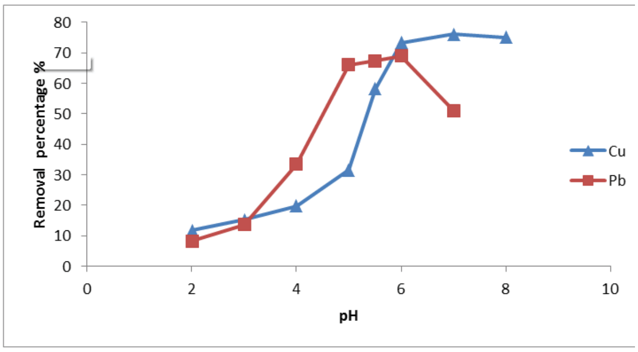

Figure 4: Effect of pH on removal percentage of Pb^{+2} and Cu^{+2} ions by nano-sawdus

Effect of pH

pH of the solution is one of the most important parameters that affect biosorption process, its influence not only the dissociation of functional groups on the active sites of the biosorbent but also the solution ion chemistry [16]. Figure 4 shows the removal of Pb^{2+} and Cu^{2+} as a function of pH, where the adsorption takes place slightly at lower pH values (pH=2-4) then the removal of the two metal ions increases with increasing pH of the solution and the maximum value was reached at pH 6 and 7 for Pb(II) and Cu(II) ions with removal percentage 69% and 75.99% respectively. At higher pH values [pH 7 for Pb(II) and pH 8 for Cu(II)], adsorption return to decrease again. The metal species, M(II); Cu(II) and Pb(II), are present in forms of M^{2+}, M(OH)$^{+}$, M(OH)2(S), etc. in water [17]. At low pH value of the solution, the active groups are protonated reducing the number of binding sites available for metal ions uptake so that the extent of Cu (II) and Pb(II) ions uptake is low in the high concentration of protons. Also at this pH values, the H^{+} ions present in the aqueous medium compete with the positively charged metal ions for adsorbing on the surface of biosorbent and a weak biosorption occurred due to strong electrostatic repulsive force between the protonated surface of nano-sawdust and positively-charged metal ions [18]. At pH (5-7) the adsorbent surface is deprotonated and negatively charge, making the sites available to the metal ions, which increasingly bind to adsorbent surface through a mechanism similar to that of exchange interactions [19]. The observed decrease of biosorption at higher pH probably due to chemical precipitation of metal ions as M(OH)$_2$ [20].

Effect of contact time

The effect of contact time on the biosorption of lead and copper ions onto nano sawdust is studied at different times ranged from 10-120 min. and optimum pH [6 for Pb(II)and 7 for Cu(II)]. Figure 5 shows that the removal of Pb^{2+} and Cu^{2+} as a function of contact time, where the removal percentage of the two metal ions increase rapidly with increasing contact time (i.e., high adsorption rate). For lead, minimum percentage removal was 43.43% at time of 10 min and it increased to maximum value 73.98% at time of 40 min, whereas, for copper, minimum value was 45.8% at time of 10 min to maximum value of 93% at time of 50 min. After maximal time, increasing in contact time is not effective in the adsorption process. The rate of the biosorption of the two metal ions onto the surface of the nano sawdust occurred in two steps. The biosorption was very fast initially as a large number of vacant surface sites are available for binding with metal ions. As the surface adsorption sites become exhausted, the uptake rate is controlled by the rate at which the adsorbate is transported from the exterior to the interior sites of the adsorbent particles. Then biosorption reached equilibrium as a result of the reduction of available sites which are difficult to be occupied due to repulsive forces between metal ions biosorbed onto the biosorbent surface and the bulk phase [16,21,22].

Effect of adsorbent dosage

Figure 6 shows the effect of changing the adsorbent dosage on the biosorption of lead and copper ions onto nano-sawdust over a range from 0.2-2 g. For lead, minimum percentage removal was 53.48% for the dose of 0.2 g and it increased to maximum value 100% for dose of 2 g, whereas, for copper, minimum value was 84.74% for the dose of 0.2 g to maximum value of 98.78% for the dose of 1 g. But the maximum adsorption of copper is attained after the dose 1 g of nano-sawdust, and hence the amount of ions bound to the adsorbent and the amount of free ions remains constant even with further addition of the dose of adsorbent. The increase in biosorption with increasing biosorbent dosage is due to increasing number of biosorbent particles thus more surface areas were available for metal ions attachment [23,24]. It can be concluded that by increasing the adsorbent dose, the availability of the exchangeable sites or surface area increases and the removal efficiency of nano-sawdust increases.

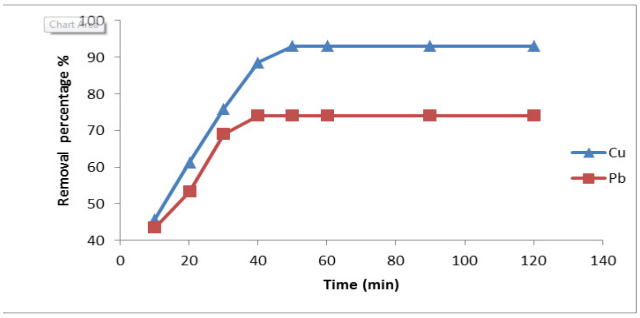

Figure 5: Effect of contact time on removal Pb^{+2} and Cu^{+2} ions by nano-sawdust.

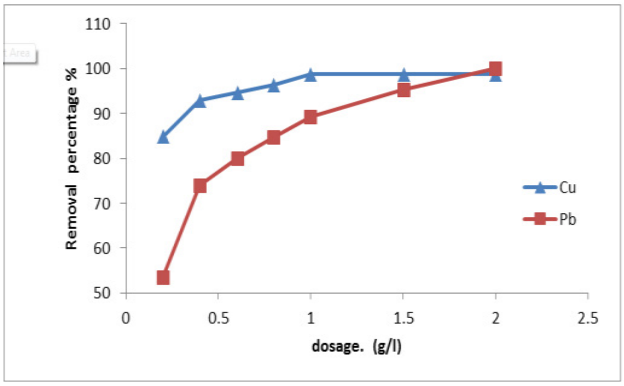

Figure 6: Effect of biosorbent dosage on removal percentage of Pb^{+2} and Cu^{+2} ions by nano-sawdust.

Effect of metal ions concentration

Figure 7 shows the effect of changing initial metals ions concentration on the biosorption of lead and copper ions on nano-sawdust over a range from 1-13 mg/l at the optimal dosage for 5 mg/L of metal ions [2 g for Pb(II) and 1 g for Cu(II)]. The initial concentration of metal ions plays an important role, as a given mass of the adsorbent can adsorb only a certain amount of the adsorbate. The more concentration of the adsorbate in solution, the smaller is the ability of the adsorbent to adsorb. In high concentration range, the fractional adsorption is low [25,26]. For lead, maximum removal (100%) was at concentration (1-5 mg/l) then decreased to minimum removal (91.68%)at concentration (13 mg/l). For copper, maximum removal (99%) was at concentration (1.3 mg/l) and decreased to minimum removal (88.46) at (13 mg/l). From data it is noted that, the biosorption of nano-sawdust decreased with the increasing of initial metal ions concentrations. By increasing the heavy metal ion concentration, the available adsorption sites are already occupied and consequent adsorption is not as efficient as in the beginning, leading to the observed decrease [27]. The biosorption percentage decrease may be due to lack of surface active sites of biosorbent to absorb the metal ions in the solution [28].

Adsorption kinetics

Adsorption is a physical-chemical process that the mass transfers a solute (adsorbate) from the fluid phase to the adsorbent surface [29]. A study of kinetics of adsorption is very important, as it provides information about the mechanism of adsorption, which is important for efficiency of the process [30]. Adsorption kinetics was studied at different contact time (10-120). Data was analyzed to detect which model is suitable explain adsorption of the two metals. Figure 8 shows pseudo-first-order model, which obtained by plotting in (q_e-q_t) against

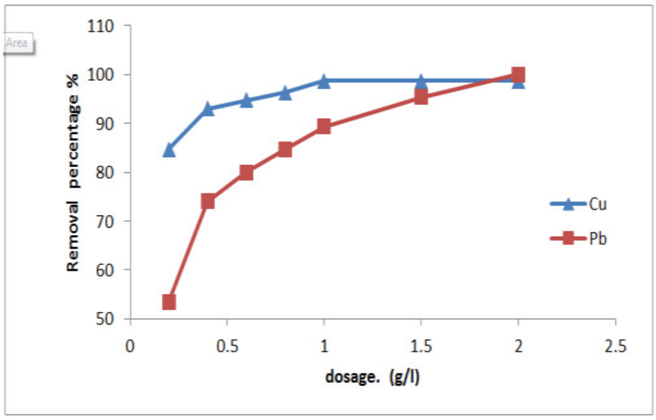

Figure 7: Effect of initial metal ion concentration removal percentage of Pb^{+2} and Cu^{+2} ions by nano-sawdust.

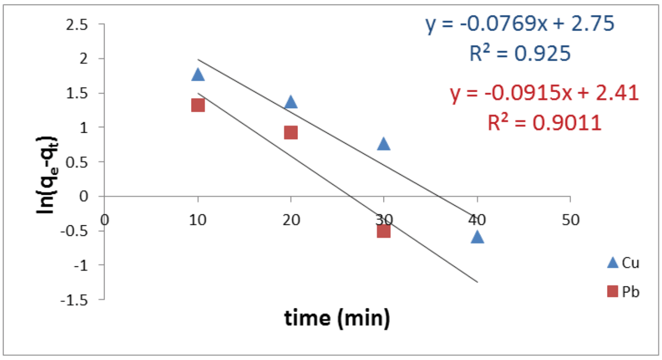

Figure 8: Pseudo-first-order reaction model for adsorptionof $Pb^{+2}$and Cu^{+2} ions on nano-sawdust.

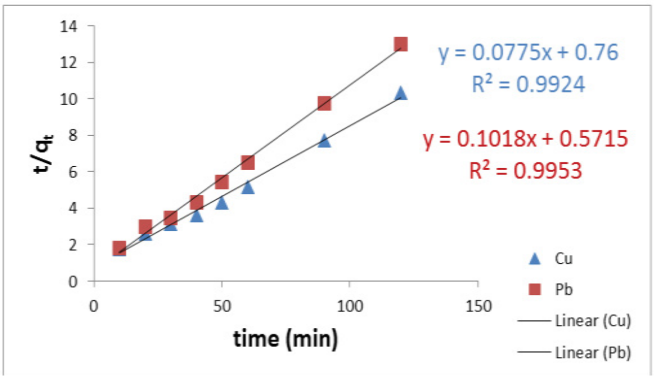

Figure 9: Pseudo-second-order reaction model for adsorptionof $Pb^{+2}$and Cu^{+2} ions on nano-sawdust.

	Pseudo-first-order				Pseudo-second-order			
Metal ions	qe (found) (mg/g)	qe (cal) (mg/g)	K1 ($L.min^{-1}$)	R2	qe (found) (mg/g)	q_e (cal) (mg/g)	$K^2(g.mg^{-1}.min^{-1})$	R^2
Pb+2	9.22	11.13	0.091	0.9	9.22	9.82	0.018	0.99
Cu+2	11.62	15.64	0.076	0.92	11.62	12.98	0.007	0.99

Table 2: Pseudo-first-order and pseudo-second -order parameters for adsorption of Pb+2 and Cu+2 ions on nano- sawdust.

time (t). The value of K_1 is the rate constant of pseudo-first-order, which obtained from the slopes of the plot. The capacity q_e is calculated from the intercepts.

Figures 8 and 9 shows that pseudo-second-order reaction model of the two metals gave very good straight lines compared to the pseudo-first-order reaction model, which is significantly nonlinear. Also by comparing the theoretical (calculated) values of q_e of the two models with the experimental value of q_e in Table 2, it shows that calculated values of q_e of pseudo-second-order reaction model for the two metals are very close to the experimental values of q_e. These facts suggest that the adsorption of the two metals by nano-sawdust follows the pseudo-second order reaction model, which relies on the assumption that chemisorption may be the rate- limiting step. In chemisorption, the heavy metals stick to the adsorbent surface by forming a chemical (usually covalent) bond and tend to find sites that maximize their coordination number with the surface. Chemisorption is usually restricted to just one layer of molecules on the surface, although it may be followed by additional layers of physically adsorbed molecules [31]. Also comparison between the correlation coefficients, R^2 of the two models for the two metals can ensure that the biosorption follows the pseudo-second -order which has higher R^2 value.

Adsorption isotherm

The equilibrium relationship between adsorbent and adsorbate are described by adsorption isotherms, usually the ratio between the quantity adsorbed and that remaining in solution at a fixed temperature at equilibrium. Adsorption isotherm was studied at varying initial metal ions concentrations (1-13 mg/L) and at constant temperature. Various isotherm models have been developed for describe how solutes interact with the sorbent, including Langmuir and Freundlich [32,33]. The Langmuir model was derived to describe monolayer adsorption of an adsorbate on a homogenous, flat surface of an adsorbent and each adsorptive site can be only occupied once in a one-on-one manner [34,35]. Figure 10 shows Langmuir models for the two metals ions by plotting C_e/q_e versus C_e. Monolayer adsorption capacity q_{max} was calculated from slope and K_L was obtained from intercept.

The Freundlich model is used to describe the adsorption of an absorbate on a heterogeneous surface of an adsorbent. Figure 11 shows Freundlich models for the two metals ions by plotting log q_e versus log C_e. The adsorption intensity 1/n, which indicates both the relative distribution of energy and the heterogeneity of the adsorbent sites, was determined from the slope and K_f was calculated from intercept.

The isotherms parameters in Table 3, pointed to that Langmuir isotherm is favorable for the two metals as R_L is greater than zero and

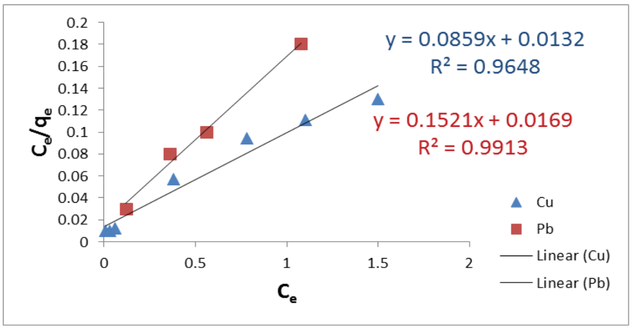

Figure 10: Langmuir adsorption isotherm for Adsorption of Cu^{+2} and Pb^{+2} ions on nano-sawdust.

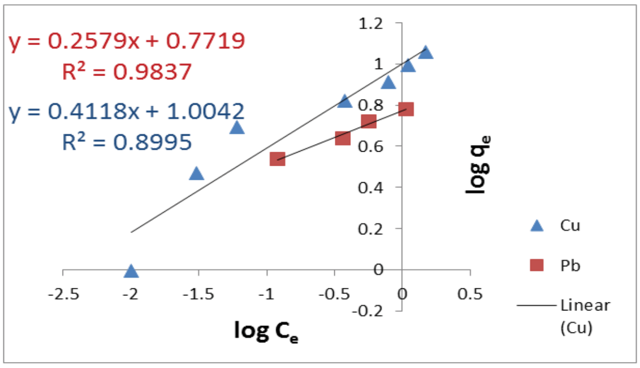

Figure 11: Freundlich adsorption isotherm for adsorption of Cu^{+2} and Pb^{+2} ions on nano- sawdust.

	Langmuir isotherm				Langmuir isotherm		
Metal ions	KL(L.mg^{-1})	qmax	RL	R2	Kf	1/n	R2
Pb(II)	9.51	6.57	0.008	0.99	5.91	0.26	0.98
Cu(II)	6.61	11.62	0.01	0.96	1.004	0.41	0.89

Table 3: Langmuir and Freundlich isotherm parameters for adsorption of Cu^{+2} and Pb^{+2} ions on nano-sawdust.

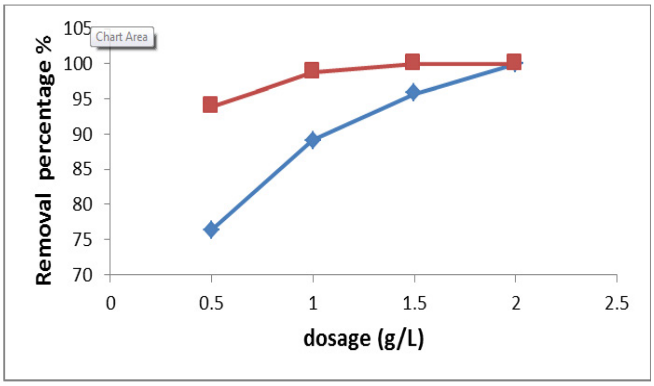

Figure 12: Effect of biosorbent dosage on removal percentage of Pb^{+2} and Cu^{+2} ions together by nano-sawdust.

Metal ions	Initial concentration	Residual concentration	Removal percentage %
Pb+2	5.0215	-	100
Cu+2	5.0201	-	100

Table 4: Removal of heavy metal ions from wastewater by nano- sawdust.

less than unity, also Freundlish isotherm is favorable as 1\n which is greater than 0.1 and less than unity. But by comparison between the correlation coefficients, R^2 of the two models indicate that the higher value of R^2 for Langmuir isotherm of the two metals as compared to Freundlich isotherm for adsorption of the two metal ions showed a better applicability of Langmuir isotherm model. This suggested that the adsorption of the two metal ions occurs on a homogeneous surface by monolayer adsorption [36].

Multi-Components System

Figure 12 shows the effect of adsorbent dose on the multi-components system, where the removal percentage of the two metal increase with increasing dosages of nano sawdust until they reach maximum removal at 2 g of the adsorbent. As indicated previously, the increase in biosorption with increasing biosorbent dosage is due to increasing number of biosorbent particles thus more surface areas were available for metal ions attachment [1].

Application on Wastewater

Nano-sawdust was used for removing metal ions from wastewater. The pH of the wastewater was adjusted to a value 6.5 according to the experimental results. Generally, the removal percentages obtained were 100% for $Pb^{+2}$and 100% for Cu^{+2}, indicating that nano-sawdust has a high removal capability towards heavy metal ions as in Table 4.

References

1. Acharya J, Sahu JN, Mohanty CR, Meikap BC (2009) Removal of lead (II) from wastewater by activated carbon developed from Tamarind wood by zinc chloride activation. J Chem Eng 149: 249-262.
2. Afkhami A, Saber-Tehrani, M, Bagheri H (2010) Simultaneous removal of heavy-metal ions in wastewater samples using nano-alumina modified with 2,4-dinitrophenylhydrazine. J Hazard Mater 181: 836-844.
3. Al-Qodah Z (2006) Biosorption of heavy metal ions from aqueous solutions by activated sludge. J Desalination 196: 164-176.
4. Bhattacharyya KG, Sharma A (2004) Adsorption of Pb(II) from aqueous solution by Azadirachta indica (neem) leaf powder. J Hazard Mater 113: 97.
5. Bourliva A, Michailidis K, Sikalidis C, Filippidis A, Betsiou M (2013) Lead removal from aqueous solutions by natural greek bentonites. J Clay Minerals 48: 771.
6. Bozic D, Stankovic V, Gorgievski M, Bogdanovic G, Kovacevi R (2009) Adsorption of heavy metal ions by sawdust of deciduous trees. J Hazard Mater 171: 684-692.
7. Cox JS, Smith DS, Warren LA, Ferris FG (1999) Characterizing heterogeneous bacterial surface functional groups using discrete affinity spectra for proton binding. J Environmental Science & Technology 33: 4514-4521.
8. Dabrowski A (2004) Selective removal of the heavy metal ions from waters and industrial wastewaters by ion-exchange method. J Chemosphere 56: 91-106.
9. Dakiky M, Khamis M, Manassra A, Mer'eb M (2002) Selective adsorption of chromium (VI) in industrial wastewater using low-cost abundantly available adsorbents. J Adv Environ Res 6: 533-540.
10. Dinu MV, Dragan ES (2008) Heavy metals adsorption on some iminodiacetate chelating resins as a function of the adsorption parameters. React Funct Polym 68: 1346-1354.
11. Dinu MV, Dragan ES, Trochimczuk AW (2009) Sorption of Pb(II) Cd(II) and Zn(II) by iminodiacetate chelating resins in non-competitive and competitive conditions. Desalination 249: 374-379.
12. Elmorsi TM (2011) Equilibrium isotherms and kinetic studies of removal of methylene blue dye by adsorption onto miswak leaves as a natural adsorbent. J Environmental Protection 2: 8-17.
13. El-Qada EN, Allen SJ, Walker GM (2006) Adsorption of methylene blue onto activated carbon produced from steam activated bituminous coal a study of equilibrium adsorption isotherm. J Chem Eng 124: 103-110.
14. Garg UK, Kaur MP, Garg VK, Sud D (2007) Removal of Hexavalent Chromium from Aqueous Solution by Agricultural Waste Biomass. J Hazard Mater 1: 40-60.
15. Gupta SS, Bhattacharyya KG (2008) Immobilization of Pb(II) Cd(II) and Ni(II) ions on kaolinite and montmorillonite surfaces from aqueous medium. J of Environmental Management 8: 7-46.
16. Haider S, Park SY (2009) Preparation of the electrospun chitosan nanofibers and their applications to the adsorption of Cu(II) and Pb(II) ions from an aqueous solution. J Membrane Sci 328: 90-96.
17. Hameed BH, Din ATM, Ahmad AL (2009) A novel agricultural waste adsorbent for the removal of cationic dye from aqueous solutions. J Hazard Mater 162: 305.
18. Hashem A, El-Khiraigy K (2013) Bioadsorption of Pb(II) onto Anethum

graveolens from Contaminated Wastewater: Equilibrium and Kinetic Studies. J Environmental Protection 4: 108.

19. Ho YS, CKay GM (1999) Pseudo-second order model for sorption processes. J Process Biochemistry 34: 735.
20. Huang SH, Chen DH (2009) Rapid removal of heavy metal cations and anions from aqueous solutions by an amino-functionalized magnetic nanoadsorbent. J Hazard Mater 163: 174 -179.
21. Jain AK, Gupta VK, Bhatnagar, A Suhas (2003) Utilization of industrial waste products as adsorbents for the removal of dyes. J Hazard Mater 101: 31-42.
22. Kampalanonwat P, Supaphol P (2010) Preparation and adsorption behavior of aminated electrospun polyacrylonitrile nanofiber mats for heavy metal ion removal. J ACS App Mat Inter 2 36: 19-3627.
23. Khan TA, Ali I, Singh VV, Sharma S (2009) Utilization of fly ash as low cost adsorbent for the removal of methylene blue malachite green and rhodamine B dyes from textile waste water. J Environmental Protection science 3: 11-22.
24. Kim DS (2003) The removal by crab shell of mixed heavy metal ions in aqueous solution. J Bioresource Technol 87: 355-357.
25. King P, Rakesh N, Beena S, Prsanna Y, Prasad VSRK (2008) Biosorption of zinc onto Syzygium cumini L Equilibrium and kinetic studies. J Chem Eng 144: 181-187.
26. Mishra PC, Patel RK (2009) Removal of lead and zinc ions from water by low cost adsorbents. J Hazard Mater 168: 319-325.
27. Navarro RR, Wada S, Tatsumi K (2005) Heavy metal precipitation by polycation-polyanion complex of PEI and its phosphonomethylated derivative. J Hazard Mater 123: 203-209.
28. Ozacar M, Ayhan Sengil I (2005) Adsorption of metal complex dyes from aqueous solutions by pine saw dust. J Bio Res Tech 96: 791-795.
29. Panayotova T, Dimova TM, Dobrevsky I (2007) Purification and reuse of heavy metals containing wastewaters from electroplating plants. J Desalination 206: 135-140.
30. Qiu H, Lv L, Pan BC, Zhang QJ, ZhangW M, et al. (2009) Critical review in adsorption kinetic models. JZhejiang University Science A 10: 7-16.
31. Saeed K, Haider S, Oh TJ, Park SY (2008) Preparation of amidoxime-modified polyacrylonitrile (PAN-oxime) nanofibers and their applications to metal ions adsorption. J Membrane Sci 322: 400-405.
32. Silva SP, Sousa S, Rodrigues J (2004) Adsorption of acid orange 7 dye in aqueous solutions by spent brewery grains. Sep Purif Technol 40: 309-315.
33. Srivastava VC, Mall ID, Mishra IM (2008) Removal of cadmium(II) and zinc(II) metal ions from binary aqueous solution by rice husk ash. Colloid Surface A 312: 172-184.
34. Vegliò F, Beolchini F (1997) Removal of metals by biosorption. J Hydrometallurgy 44: 301-316.
35. Vilar VJP, Botelho CMS, Boaventura RAR (2007) Copper desorption from Gelidium algal biomass. J Water Res 41: 1569-1579.
36. Yu LJ, Shukla SS, Dorris KL, Shukla A, Margrave JL (2003) Margrave adsorption of chromium from aqueous solutions by maple sawdust. J of Hazard Mater 10: 0- 53.